International Conference on Renewable Energies and Power Quality (ICREPQ'15)
La Coruña (Spain), 25th to 27th March, 2015
Renewable Energy and Power Quality Journal (RE&PQJ)
ISSN 2172-038 X, No.13, April 2015

Harmonic Modeling of Electric Vehicle Chargers in Frequency Domain

S. Müller[1], J. Meyer[1], P. Schegner[1], S. Djokic[2]

[1] Technische Universitaet Dresden
Institute of Electrical Power Systems and High Voltage Engineering
01062 Dresden (Germany)
e-mail: sascha.mueller@tu-dresden.de

[2] The University of Edinburgh
Edinburgh EH9 3JL, Scotland, UK
e-mail: sasa.djokic@ed.ac.uk

Abstract. Fully electric cars will be increasingly used in the near future in many countries. They are commonly known as electric vehicles (EVs) and use power electronic-based rectifiers for charging their batteries, which may significantly impact power quality in LV and MV distribution grids. Of particular importance are harmonic emissions of EV chargers, which are strongly influenced by the distortion of the supply voltage.
This paper presents the results of testing and analyzing harmonic current emission of eight different single-phase EV chargers, with respect to supply voltage distortion. The analysis is based on extensive measurements performed at a test stand, capable of accurately reproducing supply voltage waveforms with desired distortion. The harmonic model consists of a constant part and a part that depends on the level of harmonics in the supply voltage. In order to characterize each EV charger in a general model, some characteristic indices are introduced, which quantify the sensitivity and linearity of harmonic currents of EV chargers to harmonics present in the supply voltage. The paper presents and discusses results for each individual EV charger, as well as a comparison of them.

Key words

Electric Vehicles, Harmonic Analysis, Load Modeling

1. Introduction

The number of electric vehicles (EVs) in Germany is expected to strongly increase within the next decade due to the anticipated electrification of road transportation sector. The EV batteries are charged by direct current (DC), which is provided by a rectifier. Due to its topology and its control, the rectifier power electronic circuit will typically cause a distortion of charging current, which in turn can influence the distortion of the supply voltage.

To determine the impact of an increasing penetration of EVs using network simulation software, appropriate models have to be developed [1-3]. One of the most significant factors with impact on the harmonic emission of EV chargers is the background distortion of supply voltage [4]. In order to develop a comprehensive and accurate frequency domain model, the dependency of harmonic emission on different supply voltage distortions has to be analyzed for a representative set of EV chargers.

The measurements of the EV chargers are carried out using an automated test setup, which is described in Section 2, which also provides some basic information on the measuring procedure proposed by the authors for a detailed harmonic characterization. Section 3 introduces characteristic indices for evaluating harmonic current emission behavior of an EV charger with respect to the modeling process. Finally, Section 4 presents the characterization results for 8 different EV chargers with a present market share in Germany of more than 70 % [5].

2. Measurement procedure

The measurements are carried out using a test bed that comprises a three-phase grid simulator. Via a control PC, which is connected to this simulator, the voltage magnitude and waveform of a low-voltage grid can be adjusted automatically. More details can be found in [6]. The measurement of voltage and current harmonics is based on the acquisition of 10-cycle waveforms and the subsequent calculation of harmonic magnitudes and phase angles according to IEC 61000-4-7. For each testing state, a trigger signal is generated by the computer that open a new data file. This allows a simple identification to which of the predefined testing states a particular measurement data file belongs.

In order to characterize the harmonic emission of an EV charger, measurements with varying supply voltage distortion are carried out. The measuring program contains more than 3000 testing states comprising single as well as multiple harmonics that are superimposed on the fundamental supply voltage. The analysis of the impact of single voltage harmonics on the current harmonic emission is used for model development. Testing states containing multiple harmonics are intended for model verification, in particular for the validity of the superposition principle.

This paper considers only the odd harmonics of the orders 3 to 19, because these are the most important harmonics present in public low voltage grids. When testing with a single voltage harmonic, its magnitude, as well as its phase angle, is varied in 12 steps each. The results are represented as "fingerprint graphs" [7].

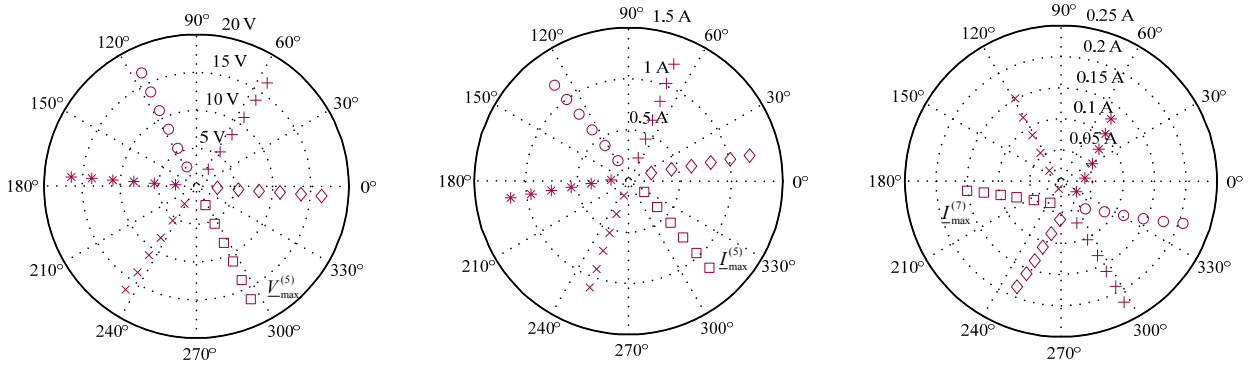

(a) 5th voltage harmonic (b) 5th current harmonic (c) 7th current harmonic

Fig. 1: Example of "fingerprint graphs", showing the impact of the 5th voltage harmonic on the 5th and 7th current harmonics

An example of the impact of the 5th voltage harmonic on the 5th current harmonic is presented in Fig. 1 (a) and (b) for 36 magnitude and phase angle combinations. A similar analysis can be carried out for voltage and current harmonics of different orders. As an example, Fig. 1 (c) shows the impact of the 5th voltage harmonic on the 7th current harmonic. While for both current harmonics the impact is almost linear, the magnitude is much higher for the current harmonic of the same order (5th), than for the adjacent odd one (7th).

3. Modeling procedure

Generally, the frequency domain model for each harmonic consists of a constant part, which is independent of supply voltage distortion and a variable part that is obtained by multiplying the voltage harmonic vector with a harmonic admittance matrix [8]:

$$\underline{I}^{(\nu)} = \underline{I}_{ref}^{(\nu)} + \underline{\mathbf{Y}} \cdot \underline{\mathbf{V}} \tag{1}$$

The constant part corresponds to the current harmonic under sinusoidal voltage supply conditions (center of the fingerprint). In order to quantify, which elements in the admittance matrix are required (representing significant impact of a specific voltage harmonic on the considered current harmonic), two indices are defined. They quantify the sensitivity of current harmonic emission depending on the level of supply voltage distortion [9]. In case of a very small sensitivity, the corresponding element in the admittance matrix can be set to zero. If the dependency cannot be neglected, another set of three indices quantifies the linearity and symmetry of the relationship between current and voltage harmonics. If the dependency is very nonlinear and/or asymmetric, the frequency domain model may not achieve the required accuracy, but it is still more accurate than a constant harmonic current model.

A. Sensitivity Indices

The sensitivity indices are defined as the ratios of harmonic currents to harmonic voltages (representing a kind of "harmonic admittances"). Here, the distinction is made between the impact of a voltage harmonic on the current harmonic of the same order, denoted as "auto-sensitivity", and the impact of a voltage harmonic on the current harmonic of a different order, denoted as "cross-sensitivity". As a result, a matrix containing all the sensitivity indices of one particular EV charger can be obtained. Although there is a high similarity, this matrix is not identical to the harmonic admittance matrix.

In order to calculate the sensitivity indices, the difference between the maximum (cf. Fig. 1) and minimum values of each branch in the fingerprint of voltage (in Volts) and the corresponding branch in the fingerprint of current (in Amps) is determined. Next, the ratio of both differences is calculated and, finally, the mean value for all branches of the fingerprint is determined. The auto-sensitivity index $S^{(\nu\nu)}$ is calculated as follows:

$$S^{(\nu\nu)} = \frac{1}{n}\sum_{i=1}^{n}\left|\frac{\underline{I}_{i\max}^{(\nu)} - \underline{I}_{i\min}^{(\nu)}}{\underline{V}_{i\max}^{(\nu)} - \underline{V}_{i\min}^{(\nu)}}\right| \cdot 1000 \tag{2}$$

Similarly, the cross-sensitivity index $S^{(\nu\mu)}$ for harmonic voltages and currents of different order can be obtained:

$$S^{(\nu\mu)} = \frac{1}{n}\sum_{i=1}^{n}\left|\frac{\underline{I}_{i\max}^{(\mu)} - \underline{I}_{i\min}^{(\mu)}}{\underline{V}_{i\max}^{(\nu)} - \underline{V}_{i\min}^{(\nu)}}\right| \cdot 1000 \tag{3}$$

The symbols ν and μ indicate the orders of the respective harmonics. In order to get more manageable values, the indices are multiplied by a factor 1000. The absolute values represent the "robustness" of the EV charger in terms of supply voltage distortion. The smaller the value, the more insensitive is the analyzed EV charger.

In order to evaluate, for which combination of harmonic voltage and current orders the sensitivity can be neglected, a suitable threshold has to be defined. For that purpose, a cluster analysis was applied to the calculated sensitivity indices of all measured EV chargers. Beside several small clusters (representing significant sensitivity), one large cluster was obtained, which can be interpreted as a "noise". It contains indices that have no significant impact on the current harmonics. A suitable empirically identified threshold to identify this cluster is selected as $S_{\mathrm{lim}}^{(\nu\mu)} = 7$. Accordingly, if a magnitude change of 1 V for a particular voltage harmonic ν results in a change of the magnitude of a current harmonic μ of less than 7 mA, the admittance for this particular combination of harmonic voltage and current order is set to zero, meaning that this cross-sensitivity can be neglected.

B. Linearity Index

The dependency between harmonic voltages and currents of different orders can be strongly nonlinear. This can have a considerable impact on the accuracy of the frequency domain model and is quantified by a linearity index.

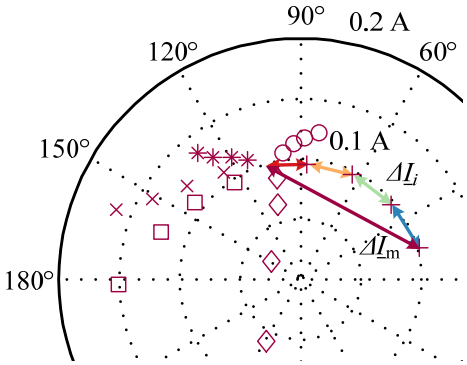

Fig. 2: Illustration of nonlinearity.

The process of calculating this index is as follows:

1. Determine the distances $\Delta \underline{I}_i$ between the successive points of each branch j (illustrated by short arrows in Fig. 2 for one branch).
2. Determine the distance $\Delta \underline{I}_\mathrm{m}$ between the maximum value and center of the fingerprint (for sinusoidal supply voltage, illustrated by long arrow in Fig. 2).
3. Calculate the ratio of $\Delta \underline{I}_\mathrm{m}$ and the sum of all single distances $\Delta \underline{I}_i$ for each branch j.
4. Calculate the 25$^{\mathrm{th}}$ percentile $Q_{0.25}$ for all branches.

The 25$^{\mathrm{th}}$ percentile is used as linearity index $L^{(\nu\mu)}$:

$$P_j\left(\frac{\Delta \underline{I}_\mathrm{m}^{(\nu\mu)}(j)}{\sum_i \Delta \underline{I}_i^{(\nu\mu)}(j)} \le Q_{0.25}\right) = 0.25\ ,\ L^{(\nu\mu)} = Q_{0.25}\ , \qquad (4)$$

In that way, the range of calculated values for the linearity index is between 0 and 1, where a value of 1 means perfect linearity, because all points are located on a line. A suitable threshold to identify sufficient linearity is selected as a value of $L_{\mathrm{lim}}^{(\nu\mu)} = 0.8$.

C. *Asymmetry Indices*

The fingerprint can be not only nonlinear, but also asymmetric. This asymmetry is described by the two further indices:

a) Asymmetry of magnitude $A_\rho^{(\nu\mu)}$

b) Asymmetry of phase angle $A_\varphi^{(\nu\mu)}$,

indicating how much a particular branch of a fingerprint differs from the others. These indices are similar to the coefficient of variation, common in empirical statistics.

Each branch of a current harmonic fingerprint consists of multiple points that correspond to respective points of the voltage harmonic fingerprint. While the distances between neighboring points in a branch of a voltage harmonic fingerprint are equal, this is not necessarily the case in the corresponding current fingerprint (Fig. 3). To determine the asymmetry of magnitude, for each branch the differences $\Delta \underline{I}_j$ between neighboring points are calculated. In Fig. 3, this is illustrated using examples of the distances between the two outmost values of each branch of the current fingerprint. For each "group", the standard deviation $s_{\rho j}$ of all distances is divided by their mean value. Then, the 75$^{\mathrm{th}}$ percentile of all ratios is compared with the threshold $A_{\rho\,\mathrm{lim}}^{(\nu\mu)} = 1$, where smaller values indicate a sufficient symmetry in terms of magnitude.

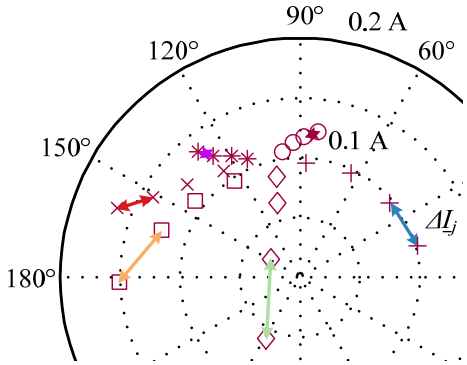

Fig. 3: Illustration of magnitude asymmetry.

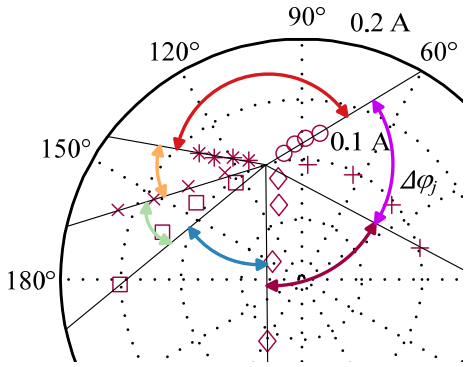

Fig. 4: Illustration of phase angle asymmetry.

$$P_i\left(\frac{s_{\rho j}^{(\nu\mu)}(i)}{\overline{\Delta \underline{I}_j^{(\nu\mu)}}(i)} \le Q_{0.75}\right) = 0.75\ ,\ A_\rho^{(\nu\mu)} = Q_{0.75} \qquad (5)$$

The index $A_\varphi^{(\nu\mu)}$ is obtained in a similar way, but phase angle differences instead of magnitude differences are used. In Fig. 4 the angle differences between the lines connecting the first and last values in two successive branches are indicated as an illustration. The phase angles between the neighboring lines are used to calculate all ratios. Finally the 75$^{\mathrm{th}}$ percentile of the ratios is compared to $A_{\varphi\,\mathrm{lim}}^{(\nu\mu)} = 1$:

$$P_i\left(\frac{s_{\varphi j}^{(\nu\mu)}(i)}{\overline{\Delta\varphi_j^{(\nu\mu)}}(i)} \le Q_{0.75}\right) = 0.75\ ,\ A_\varphi^{(\nu\mu)} = Q_{0.75} \qquad (6)$$

Again larger values mean increased asymmetry, while values below 1 indicate a sufficient symmetry in terms of phase angle. The thresholds were obtained empirically: 25$^{\mathrm{th}}$ percentile and 75$^{\mathrm{th}}$ percentiles, respectively, are more robust estimators compared to e.g. use of the minimum or maximum values.

D. *Generation of admittance matrix*

The flowchart in Fig. 5 illustrates the determination of the non-zero elements of the harmonic admittance matrix. In the first step, Stage (1), the sensitivity index is evaluated. If it is higher than the threshold, the impact of the considered voltage harmonic on the specific current harmonic cannot be neglected. In the second step, Stage (2), the linearity and asymmetry indices are calculated, and if they meet with their respective limits, the admittance is set to the sensitivity index, otherwise it is set to zero.

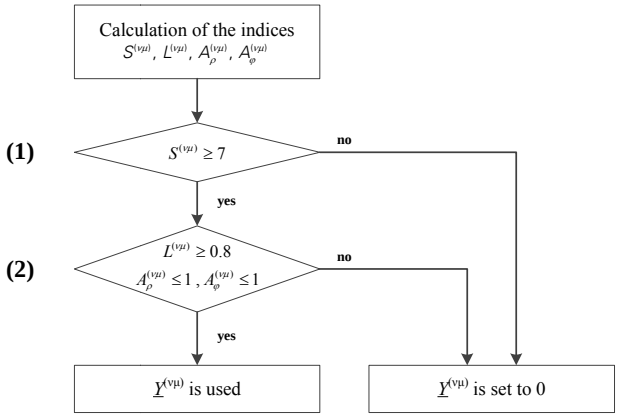

Fig. 5: Flowchart for determination of the elements of the harmonic admittance matrix (including μ=ν).

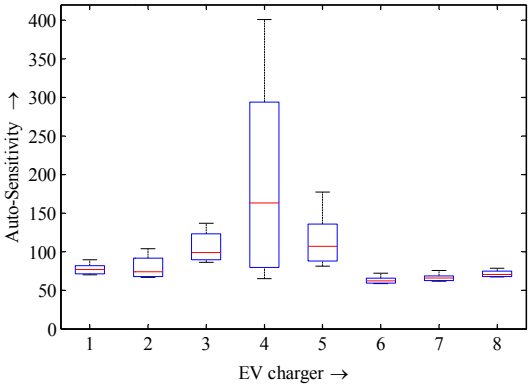

Fig. 6: Auto-sensitivity indices.

4. Results

The results for all eight analyzed EV chargers are discussed with respect to the indices introduced in Section 3. In the following text, the EV chargers are compared with each other to evaluate similarities and differences in their harmonic emission behavior. Only the elements that remain non-zero after applying the flowchart in Fig. 5 are considered. Box-Whisker plots are used to indicate the range of variation. The actual ranges of values are indicated with black bars, while upper and lower sides of the blue rectangles correspond to the 75th and 25th percentile, respectively, and the median is indicated by a red line. Values, which are located outside four times the interquartiles range, are defined as outliers and marked by red crosses.

A. Sensitivity Indices

The *auto-sensitivity* indices, i.e. the diagonal elements of the admittance matrix, are always present. As there are nine harmonic orders (from 3rd to 19th), nine auto-sensitivity indices can be calculated for each EV. Fig. 6 shows the variation ranges of the auto-sensitivity indices of all eight EVs, with the overall median value around $S^{(\nu\nu)} = 100$. The following can be concluded:

- All EV chargers are sensitive to voltage harmonics. Constant harmonic current source models are therefore not adequate for their modelling.
- The EV chargers show different behavior, which would require different models with different parameters for realistic studies.
- With a median auto-sensitivity value of around $\overline{S}^{(\nu\nu)} > 150$ and the largest variation range, EV charger 4 is the most sensitive one.
- The ranges of variation and sensitivity are smallest for the EV chargers 1, 6, 7 and 8

In case of the cross-sensitivity indices, only the elements with $S^{(\nu\mu)} > S_{\text{lim}}^{(\nu\mu)}$ are taken into account, resulting in different numbers of these elements for different EV chargers. In order to better understand which of the matrix elements must be considered, the sensitivity matrix is visualized using intensity plots in Fig. 7. Dark colors indicate higher sensitivity, while elements colored in yellow or white ($S < 7$) are set to zero. All indices (including the auto-sensitivity indices) with $S > 20$ are marked black.

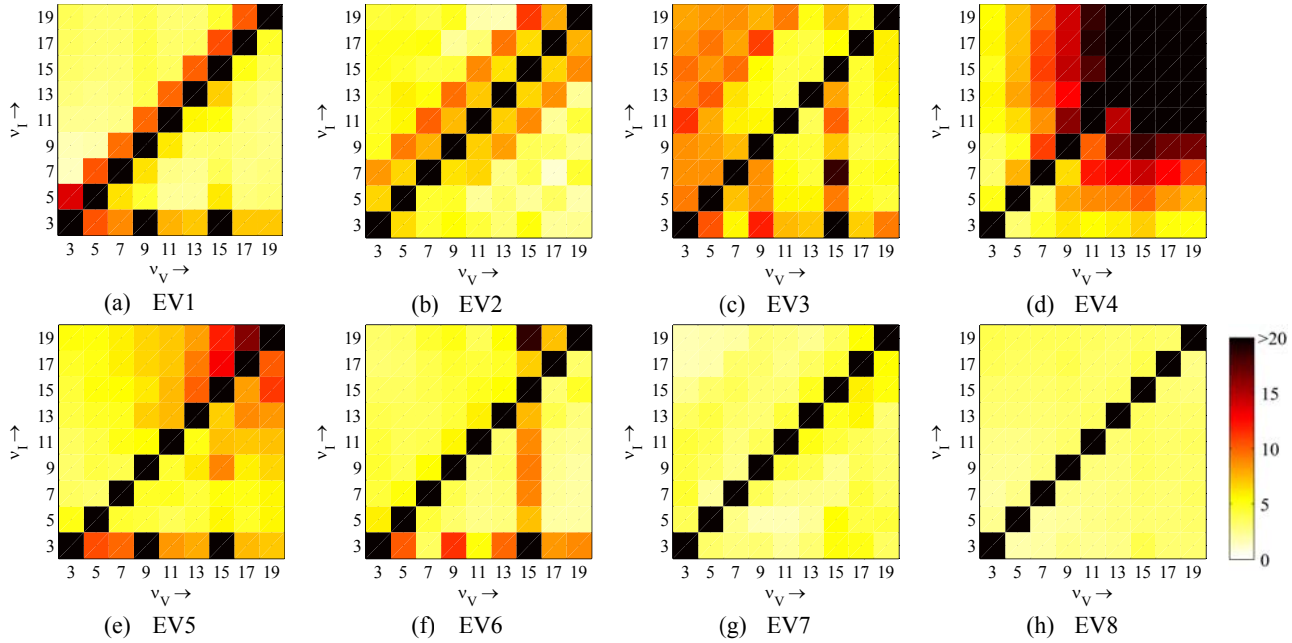

Fig. 7: Sensitivity indices (i.e. harmonic admittances) of measured EV chargers; color corresponds to the calculated magnitude values.

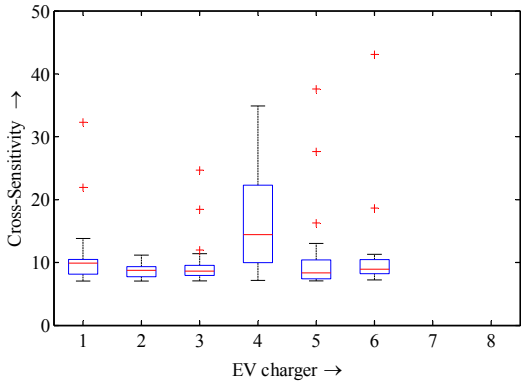

Fig. 8: Cross-sensitivity indices.

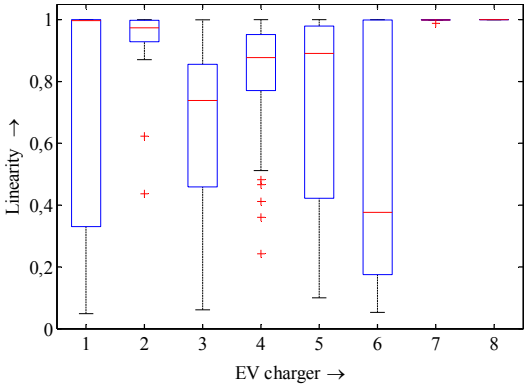

Fig. 9: Linearity index.

Based on the plots in Fig. 7, the EV chargers can be separated into four different groups with distinctively different behavior:

- EVs 7 and 8: No dependency between voltage and current harmonics of different orders.
- EV 2: Only elements adjacent to the diagonal elements (distance of two or four harmonic orders) have to be considered.
- EVs 1, 3, 5, 6: The 3rd current harmonic is particularly sensitive to the 9th and 15th voltage harmonics. In addition, the 15th voltage harmonic also influences some or all other current harmonics.
- EV 4: The sensitivity increases with the harmonic order of voltage and current and is not only limited to the elements adjacent to the diagonal.

The variation range of the cross-sensitivity indices is shown in Fig. 8. Again, EV 4 has the most sensitive charger. EVs 7 and 8 are not displayed, because no cross-sensitivity exists. For all other EVs (1, 2, 3, 5, 6), the median value is around $S^{(v\mu)} = 10$, which is about one-tenth of the overall median of the auto-sensitivity $S^{(vv)}$ for the tested EV chargers.

To estimate what accuracy can be expected by the model based on the parameterization by auto- and cross-sensitivity indices, linearity and asymmetry indices has to be evaluated.

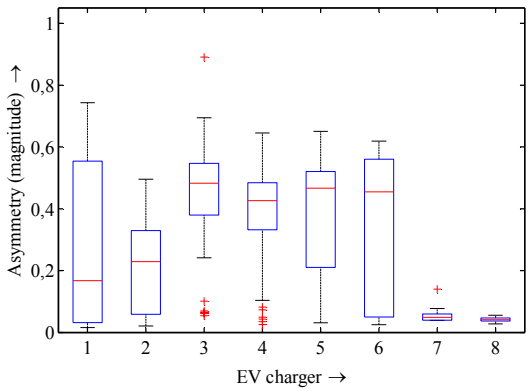

Fig. 10: Asymmetry of magnitude.

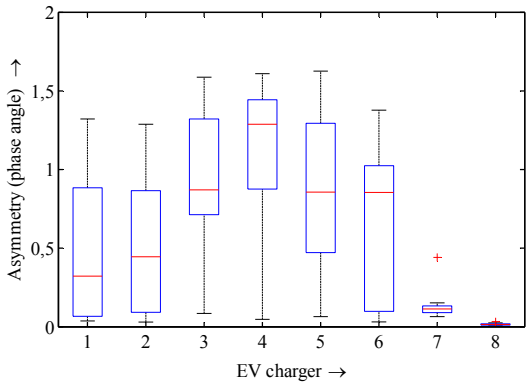

Fig. 11: Asymmetry of phase angle.

B. *Linearity Index*

Linearity is specified as sufficient if this index value is higher than $L = 0.8$. The box plot of the variation ranges is shown in Fig. 9:

- EVs 1, 3, 5 and 6 (one of the groups in previous section) have a large variation of linearity index with a considerable amount of values below the threshold.
- EVs 2 and 4 show only some small non-linearities, but within the allowed value range. EV 2 has the smallest range of variation, i.e. it behaves in the most linear way.
- EVs 7 and 8 have linearity indices of about 1, because no cross-sensitivity exists for those EVs and auto-sensitivity is usually strongly linear.

C. *Asymmetry Indices*

The box plots for amplitude asymmetry and phase angle asymmetry are presented in Fig. 10 and 11. In cases, when this index is lower then $A = 1$, the symmetry of the respective combination of harmonic voltage and current is sufficient. By analyzing the plots, the following can be concluded:

- The asymmetry of phase angle is about two times higher than the asymmetry of magnitude.
- The threshold of magnitude asymmetry is never exceeded. All chargers have values clearly below $A_\rho = 1$.
- EVs 3, 4 and 5 show phase angle asymmetries above 1.
- EVs 7 and 8 have almost no asymmetry, because only the auto-sensitivity is featured in the admittance matrices.

D. Final admittance matrices

Applying the thresholds for the sensitivity indices (stage (1) in Fig. 5) reduces the number of elements in the admittance matrices for all EVs considerably. Depending on non-linearities of the relationships between harmonic voltages and currents, the number of elements is further decreased, if at least one of the three indices quantifying linearity and symmetry exceeds the respective threshold (stage (2) in Fig. 5).

The number of elements remaining after the first and second stage is illustrated in Fig. 12. As nine orders of voltage and current harmonics are considered for modeling, the whole matrix consists of 81 elements. The minimum number is nine, as the diagonal auto-sensitivity elements are always present. For EVs 7 and 8, no further reduction is observed in stage (2), which suggests a high accuracy of the model. For EVs 1 and 2, whose current harmonics are mainly influenced by voltage harmonics of adjacent orders, only a few elements are further excluded in stage (2), suggesting that model from eqn. (1) should be sufficiently accurate. In contrast, a highly nonlinear behavior is observed for EVs 3 to 6, for which majority of elements is removed by stage (2). In this case, a higher model error is expected.

5. Conclusion

This paper characterizes and quantifies the impact of the harmonics typically present in the supply voltage (odd harmonics between the 3rd and 19th order) on harmonic current emission for eight different EV types, which are presently commonly used in Germany. Based on measurements, the harmonic emission behavior is characterized with respect to the parameterization of a frequency domain model. Newly introduced indices for sensitivity, linearity and asymmetry allow the detailed quantification of the harmonic current behavior.

The results show a significant dependency of the harmonic current emission on the voltage distortion. Therefore, in most cases it is not sufficient to use a simple constant harmonic current source model. Moreover, the qualitatively different behavior of different EV chargers would require the implementation of various individual EV charger models, each with specific parameter sets. Even though the technology of EV chargers (active PFC) is similar, the use of a single generic model is not expected to be sufficient.

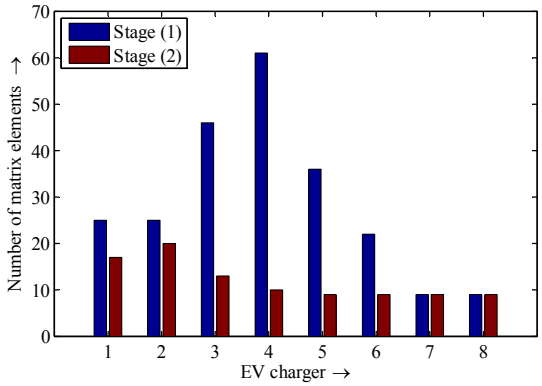

Fig. 12: Number of remaining elements in the admittance matrix

The eight different EV chargers have been classified into four groups according to their sensitivity to harmonics in the supply voltage. For some chargers, only the dependency between harmonic voltages and currents of the same order must be considered. In other cases, so called cross-sensitivities between harmonic voltages and currents of different orders have to be additionally considered. For 50 % of the tested EV chargers, the presented model is expected to be highly accurate, while for the rest the model error could be slightly higher, but still smaller than if only constant current sources are used. A preliminary verification for selected testing states with multiple harmonics has shown a good match between the simulation and measurement results, with only small errors.

The presented set of indices could be easily used to assess the behaviour of EV chargers with respect to supply voltage distortion and for classification of chargers according to their operation principles. The presented methodology can be also applied to three-phase type of EV chargers, as well as to other devices, such as photovoltaic inverters and power electronic-based general massmarket appliances.

Acknowledgement

The authors thank the German Federal Ministry for the Environment, Nature Conservation, Building and Nuclear Safety for their financial support (project: ElmoNetQ, FKZ: 16EM1052).

References

[1] A. Collin, S. Djokic, H. Thomas and J. Meyer, “Modelling of Electric Vehicle Chargers for Power System Analysis”, EPQU, Lisbon, 2011.

[2] X. Xiao, H. Molin, S. Djokic, J. Meyer et al., “Component-based Modelling of EV Battery Chargers”, Abstract accepted for presentation at PowerTech, Eindhoven, 2015.

[3] C. Jiang, R. Torquato, D. Salles and W. Xu, “Method to Assess the Power-Quality Impact of Plug-in Electric Vehicles”, IEEE Transcations on Power Delivery, Vol. 29, No. 2, 2014.

[4] A. Mansoor, W. M. Grady, R. S. Thallam, M. T. Doyle et al., “Effect of Supply Voltage Harmonics on the Input Current of Single-Phase Diode Bridge Rectifier Loads”, IEEE Transactions on Power Delivery, Vol. 10, No. 3, 1995.

[5] German Federal Office of Motor Traffic, 04/2014

[6] F. Möller, J. Meyer and P. Schegner, “Load Model of Electric Vehicles Chargers for Load Flow and Unbalance Studies”, PQ2014, Rakvere (Estonia), 2014.

[7] S. Cobben, W. Kling and J. Myrzik, “The Making and Purpose of Harmonic Fingerprints”, 19th CIRED Conference, Vienna, 2007.

[8] A. S. Fölting, J. M. A. Myrzik, T. Wiesner et al., “Practical Implementation of the Coupled Norton Approach for Nonlinear Harmonic Models”, PSCC, Wroclaw, 2014.

[9] S. Müller, J. Meyer and P. Schegner, “Characterization of Small Photovoltaic Inverters for Harmonic Modeling”, ICHQP, Bucharest (Romania), 2014.